Rotational excitation of HF in slow collisions with He†

Lee A. Collins* and Neal F. Lane

Physics Department, Rice University, Houston, Texas 77001

(Received 7 January 1975)

Low-energy rotational-excitation cross sections have been calculated from model-potential surfaces constructed to represent the interaction of atomic helium with hydrogen fluoride (HF). Quantum-mechanical solutions of the coupled equations were obtained including as many rotational states (open and closed) as needed for convergence. The behavior of the cross sections as a function of energy and the sensitivity to various model-potential surfaces are discussed.

I. INTRODUCTION

Recent interest in collisions between atoms and diatomic hydrides has arisen in such diverse fields as laser physics and astrophysics. For instance, rotational excitation of certain hydrides, in particular hydrogen chloride, by collisions with helium and molecular hydrogen appears to form an important cooling mechanism in the dense interstellar clouds.[1] In laser physics, the hydrogen fluoride laser appears to offer the prospect of a rather high yield device[2] which may have applications to fusion research. In studies aimed at increasing the efficiency of such a device, detailed knowledge of such quenching mechanisms as rotational de-excitation is needed.[2,3] In this paper, we present the results of quantum-mechanical close-coupling calculations of the cross sections for rotational excitation of the lowest few rotational levels of hydrogen fluoride (HF) by collisions with ground-state helium (He) atoms. The details of these calculations are presented in the following sections. Beginning with Sec. II, we describe a method for generating a model potential surface for this system. This is followed in Sec. III by a brief description of the methods employed for determining the cross sections. Finally, we present and discuss the results of these calculations in Sec. IV.

II. POTENTIAL SURFACE

A simple procedure has been developed for modeling the interaction surface between an incident helium atom and target diatomic molecule. The potential is divided into long- and short-range regions as

$$V(R,\Theta) = V^S(R,\Theta) + V^L(R,\Theta), \qquad (1)$$

where $\vec{R}$ is the relative position vector for the centers of mass of the interacting particles and Θ is the orientation of R with respect to the figure axis of the molecule.

The short-range part of the potential $V^S(R,\Theta)$ is modeled by averaging an electron-atom effective potential V^{eff} over the charge density of the molecule. This procedure is a generalization of a method used previously by Hickman and Lane[4] for atom-atom interactions. We chose the effective potential to resemble the electron-atom pseudopotential of Kestner et al.[5] This potential contains exchange, Coulomb, and kinetic contributions for a single electron interacting with the atom. Previous studies[4] have indicated that the general features of this interaction can be represented by the analytical expression

$$V^{\text{eff}}(s) = -(2/s)e^{-as} + b e^{-s^2/2\sigma^2}, \qquad (2)$$

where s is the electron-helium separation, related to r and ϑ by $s^2 = R^2 + r^2 - 2rR\cos\vartheta$ (see Fig. 1), and a, b, and σ are adjustable parameters. This effective potential is then averaged over the unperturbed one-electron charge density of the molecule $\rho(\vec{r})$ to obtain the interaction of all molecular electrons with the incident atom as

$$V^S(R,\Theta) = 2\pi \int\int V^{\text{eff}}(s)\rho(r,\theta)r^2 \sin\theta \, dr \, d\theta. \qquad (3)$$

The integration over the azimuthal angle ϕ has been carried out explicitly since the surface exhibits cylindrical symmetry. This potential surface is then expanded in a Legendre series of the form

$$V^S(R,\Theta) = \sum_\lambda v_\lambda^S(R)P_\lambda(\cos\Theta), \qquad (4a)$$

with

$$v_\lambda^S(R) = \frac{2\lambda+1}{2} \int_0^\pi V^S(R,\Theta)P_\lambda(\cos\Theta)\sin\Theta \, d\Theta. \qquad (4b)$$

Equation (4b) may be placed in a more tractable form by expanding ρ and V^{eff} in Legendre series of $\cos\theta$ and $\cos\vartheta$, respectively, with the radial ex-
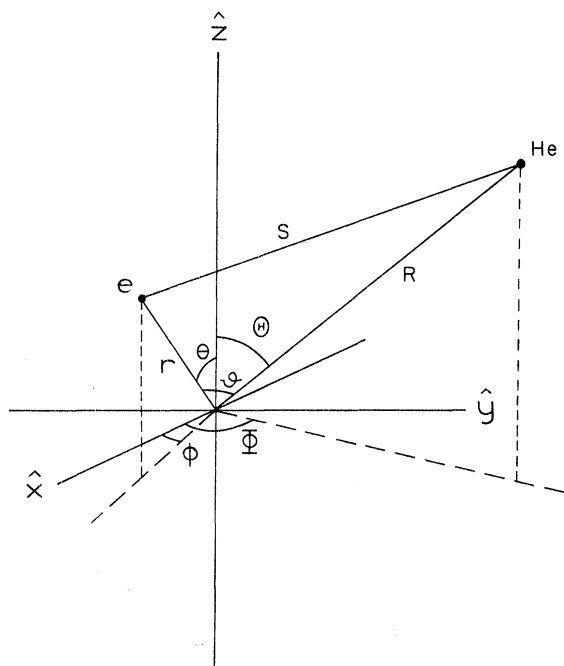
Fig. 1. Geometry of the interaction of a molecular electron with coordinates (r, θ, ϕ) and a helium atom at position (R, Θ, Φ).

pansion coefficients given by $a_\lambda(r)$ for the charge density and $\bar{v}_\lambda(R, r)$ for the effective potential. By using the addition theorem of spherical harmonics, $v_\lambda^S(R)$ can be expressed as

$$v_\lambda^S(R) = \frac{4\pi}{2\lambda + 1} \int_0^\infty a_\lambda(r) \bar{v}_\lambda(r, R) r^2 \, dr. \tag{5}$$

The $a_\lambda(r)$ coefficients must be determined by numerical quadrature; however, the $\bar{v}_\lambda(R, r)$ terms have convenient analytical forms.[6] The radial expansion coefficients are then fit to the exponential form

$$v_\lambda^S(R) = A_\lambda e^{-\alpha_\lambda R}. \tag{6}$$

The fit is made in a region where v_λ is monotonically decreasing with increasing R. Although the above method was derived for atom-molecule systems, the procedure works equally as well for atom-atom interactions. In this case, the interaction potential depends only on R and is given by Eq. (5) with λ equal to zero; $a_0(r)$ then becomes the charge density of the target atom.

The short-range interaction surface obtained by this method includes Coulomb, exchange, and kinetic contributions for the interaction of the molecular electrons with the atom. The nuclear repulsion term, the interaction between the atomic electrons and molecular nuclei, and correlation effects are neglected. Although the nuclear repul-

sion and atomic-electron–molecular-nuclei terms are large, they contribute to the energy with opposite signs and, for small tightly bound atomic systems, approximately cancel. Therefore neglecting these terms in interactions between molecules and a small closed-shell atom such as helium does not introduce serious errors. However, for interactions involving larger atoms, this technique is less suitable. Since we have also neglected correlation effects, the method best approximates the interaction in the region of small charge overlap. However, we find that a $v_\lambda^S(R)$ approximated by a fit to Eq. (6) does give reasonable results for small intermolecular separations. It should be noted that since the unperturbed charge density is used the method is applicable only to closed-shell systems.

We have applied the above procedure to the He-HF system. An appropriate effective potential was determined by fixing the parameters a, b, and σ independent of the HF system. Since *ab initio* potentials were available for He-He interactions,[7,8] the parameters were varied until the resulting potential curve agreed to within 10% of these more detailed calculations in the region beyond $3.0a_0$. This effective potential was then used in Eq. (5) along with the Hartree-Fock charge density of HF,[9] to determine the He-HF interaction surface. The v_λ^S coefficients were fit to the exponential form of Eq. (6) in the region between four and five Bohr radii (4–5 a_0). The appropriate values of A_λ and α_λ for the first five short-range radial expansion coefficients are given in Table I. Finally, in Fig. 2, we compare several of the radial coefficients of the surface with those determined from the more detailed *ab initio* restricted Hartree-Fock (RHF) potential surface recently calculated by Bender.[10] The rather good agreement leads us to believe that the effective-potential method provides a rapid, economical procedure for calculating interaction potentials between a closed-shell molecule and tightly bound atom provided the electron-atom pseudopotential and molecular charge density are known. Thus the effective-potential method complements other

TABLE I. Parameters (in atomic units) of the model He-HF potential surface.

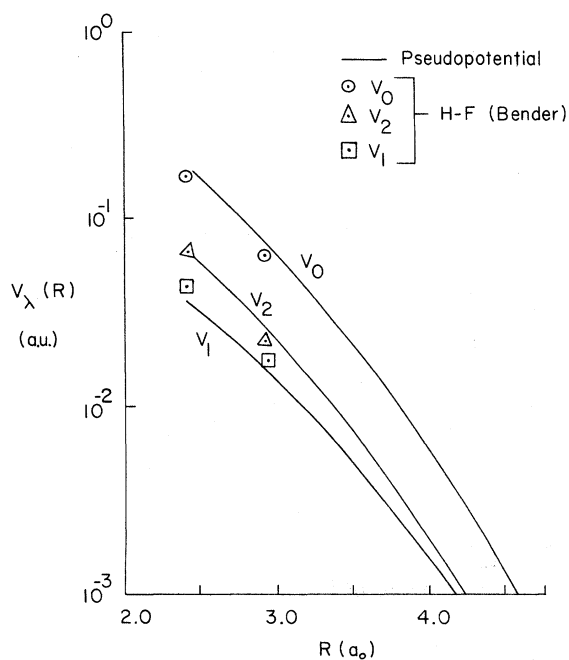| Coefficient	A_λ	α_λ	C_λ
v_0	128.275	2.494	3.42
v_1	10.356	2.151	6.78
v_2	29.253	2.379	1.55
v_3	10.739	2.173	1.41
v_4	3.875	2.115	1.23

Fig. 2. First three short-range radial expansion coefficients $v_\lambda^S(R)$ for the He-HF system as a function of intermolecular separation R. Comparison is made between the restricted Hartree-Fock calculations of Bender ($\odot$, $\square$, $\triangle$) and the effective-potential (pseudopotential) method (solid line) developed in the text.

approximate procedures for generating interaction potentials such as the Gordon-Kim method (see Ref. 7 and references therein), which has the added advantage that it can be easily extended to larger atomic systems.

The long-range part of the potential surface was also expanded in a Legendre series in $\cos\Theta$. The radial expansion coefficients $v_\lambda^L(R)$ were taken to have the form

$$v_\lambda^L(R) = -C_\lambda R^{-m}, \tag{7}$$

where m was set to 6 for v_0 and v_2, to 7 for v_1 and v_3, and to 8 for v_4. Buckingham[11] has shown that for the case of a spherical atom interacting with a polar molecule the C_λ terms may be expressed in terms of the atomic and molecular static dipole and quadrupole polarizabilities (α_{He}, $\alpha_{HF,\parallel}$, $\alpha_{HF,\perp}$, $A_{HF,\parallel}$, and $A_{HF,\perp}$), permanent dipole and quadrupole moments (μ_{HF} and Q_{HF}), and ionization energies (I_{HF}, I_{He}). Both dispersion and induction contributions are included in this expression.

For the He-HF system, we have considered only induction contributions to v_3 and v_4. In addition, the dispersion term in v_1 has been represented by an approximation in terms of the dis-

placement d of the centers of mass and charge within the molecule.[12] The parameters used in this study were as follows: $\alpha_{HF,\perp} = 2.48$[13]; $\alpha_{HF,\parallel} = 5.34$[13]; $\alpha_{He} = 1.42$[14]; $\mu_{HF} = 0.765$[15]; $Q_{HF} = 0.541$[16]; $I_{He} = 0.904$; $I_{HF} = 0.581$[9]; and $d = 0.2$. All quantities are given in atomic units (a.u.) and referred to the center of mass of the appropriate system. The values of the C_λ terms are presented in the last column of Table I.

The total radial expansion coefficient $v_\lambda(R)$ is given by the function

$$v_\lambda(R) = v_\lambda^S(R) + v_\lambda^L(R). \tag{8}$$

To avoid the singularity in the long-range part at small values of R, $v_\lambda^L(R)$ was truncated by the factor $1 - \exp[-(R/R_0)^m]$. The resulting potential interaction surface for He-HF is given in Fig. 3 for $R_0 \ll 1$. The surface is rather asymmetric, with the nonspherical terms v_1, v_2, and v_3 making comparable contributions. The coefficient v_3 closely parallels v_1, while the term v_4 is a factor of 2 or more smaller than any of the first three nonspherical terms. Both v_3 and v_4 are omitted from Fig. 3 for reasons of clarity. Higher-order terms ($\lambda > 4$) make successively smaller contributions and can be neglected in calculations involving the lowest few rotational levels ($j \leqslant 3$). Since the spherical term v_0 is somewhat stronger overall than the nonspherical ones, we consider this a case of intermediate anisotropy, hence inter-
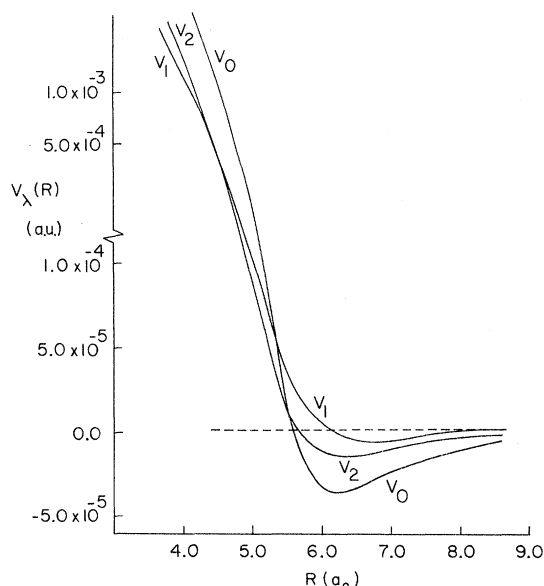

Fig. 3. Radial expansion coefficients for the He-HF potential surface as a function of intermolecular separation R. v_3 closely parallels v_1, and v_4 is a factor of 2 smaller than v_3. v_3 and v_4 are omitted for clarity.

mediate coupling. In contrast, a weak anisotropy corresponds to the case where the spherical term is much larger than the nonspherical components, while a strong anisotropy implies one or more of the nonspherical terms becomes larger than v_0.

III. SCATTERING FORMALISM

The rotational excitation cross sections for He-HF collisions were calculated within the close-coupling formulation of Arthurs and Dalgarno,[17] with HF treated as a linear rigid rotor. The resulting set of coupled equations was solved numerically by the integral-equations technique of Sams and Kouri.[18] At each value of the total energy, the cross sections were calculated using a particular basis of rotational states. Both open and closed channels were included. The size of this basis was increased until successive values of the cross section agreed to within better than 5%. For energies below 0.05 eV, four basis states were adequate for convergence; however, above this energy, as many as seven states were needed. The results of these calculations are presented in the next section.

IV. RESULTS AND DISCUSSION

Total cross sections for transitions between the lowest few rotational levels of HF in collisions with He were calculated at energies of 0.017, 0.025, 0.05, 0.10, and 0.15 eV. The results are summarized in Table II. In Fig. 4, we present the cross sections $\sigma^J(j \rightarrow j')$ for excitation from the ground rotational state, $j = 0$, to the three lowest excited states of HF as a function of total angular momentum J at an energy of 0.05 eV. We recall that $\vec{J}$ is formed by coupling the orbital angular momentum $\vec{l}$ of the incident atom and rotational angular momentum $\vec{j}$ of the molecule. In this sense the $\sigma^J(j \rightarrow j')$ may be loosely regarded as a partial-wave decomposition of the total cross section $\sigma(j \rightarrow j')$.[19]

We have tested the sensitivity of the cross sections to the manner in which the long- and short-range parts of the potential surface were merged by varying the parameters R_0 and m. These parameters determine how far the long-range term penetrates into the short-range region. We fix m at 6 and consider the following two cases: (i) R_0 very small ($\ll 1$); (ii) $R_0 = 5.0a_0$. The first case, corresponding to the solid curves in Fig. 4, represents calculations made with an untruncated (i.e., $R_0 \rightarrow 0$) long-range term. The crosses, on the other hand, denote values of the cross sections calculated for a potential whose long-range part was truncated somewhat with R_0 chosen near the zero of the spherical component v_0. The two sets of cross sections differ by less than 25%, indicating that the total cross sections are only mildly sensitive to the manner in which the two parts of the surface are joined. The potential surface of case (i) was used to determine all cross sections reported in Table II.

Another important feature of Fig. 4 is the relative strengths of the rotational cross sections. In a case of a weak or intermediate strength potential, the ordering of the cross sections roughly follows the relative magnitudes of the coupling matrix elements which directly connect the initial and final states. Since the nonspherical radial components are comparable in magnitude, the variation in coupling between states is due mainly to the Percival-Seaton (PS) coefficients,[17] which represent the angular integral in the coupling matrix element. Thus the ordering observed in Fig. 4 is expected, since the PS coefficients between the ground and higher rotational states j' decrease as j' increases. The actual relative magnitudes of these cross sections depend on the complicated interplay between all coupled channels. An investigation of Table II reveals that the relative im-

TABLE II. Rotational excitation cross sections (in units of a_0^2) vs energy (in eV) for He-HF.

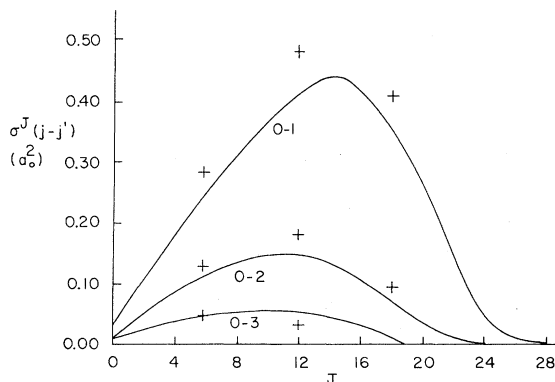| E	σ_{0-1}	σ_{0-2}	σ_{0-3}	σ_{1-2}	σ_{1-3}	σ_{2-3}
0.017	3.8	0.2	···	0.7	···	···
0.025	4.9	0.7	···	2.7	···	···
0.050	6.5	2.0	0.6	5.7	0.9	3.4
0.100	7.5	3.5	2.0	7.0	2.4	6.3
0.150	7.4	4.4	2.7	7.2	3.3	7.1

Fig. 4. Partial rotational excitation cross sections $\sigma^J(j \rightarrow j')$ as a function of J for an energy of 0.05 eV. The solid curve represents a long-range cutoff with $R_0 \ll 1$ and $m = 6$. Crosses (+) represent a long-range cutoff with $R_0 = 5.0a_0$ and $m = 6$.

portance of the cross sections for transitions to high rotational levels grows with increasing energy. Thus excitation to, or de-excitation from, high rotational levels may prove to be important in causing a redistribution of rotational populations.

We have presented a simple procedure for determining the interaction potential surface between closed-shell systems, which has been applied to the case of helium collisions with hydrogen fluoride. Using this potential surface, total rotational excitation cross sections were calculated at several energies within the close-coupling formulation including as many channels (open or closed) as needed for convergence. The sensitivity of the cross sections to changes in the model surface has also been investigated. The strengths of the cross sections for excitations to high rotor states indicate that these processes must be included in any detailed study of relaxation mechanisms. In a future paper,[20] we shall study trends encountered in going from one hydride system to another by presenting rotational excitation cross sections for collisions between helium and such hydrides as DF, HCl, and DCl. In addition, we shall investigate various approximation techniques applied to the coupled equations and their applicability to these systems.

---

†Supported in part by the U.S. Atomic Energy Commission and the Robert A. Welch Foundation.

*Part of this work was completed while the author was a summer research student at the Lawrence Livermore Laboratories.

[1] A. Dalgarno, T. deJong, M. Oppenheimer, and J. H. Black, Astrophys. J. **192**, L37 (1974).

[2] Hao-Lin Chen, R. L. Taylor, T. Wilson, P. Lewis, and W. Fyfe, J. Chem. Phys. **61**, 306 (1974), and references therein.

[3] E. Cuellar, J. H. Parker, and G. C. Primentel, J. Chem. Phys. **61**, 422 (1974).

[4] A. P. Hickman and N. F. Lane, Phys. Rev. Lett. **26**, 1216 (1971).

[5] N. R. Kestner, J. Jortner, M. H. Cohen, and S. A. Rice, Phys. Rev. **140**, A50 (1965).

[6] A. P. Hickman, M.A. thesis (Rice University, 1971) (unpublished).

[7] J. S. Cohen and R. T. Pack, J. Chem. Phys. **61**, 2372 (1974).

[8] B. Liu and A. D. McLean, J. Chem. Phys. **59**, 4557 (1973).

[9] P. L. Cade and W. M. Huo, J. Chem. Phys. **47**, 614 (1967).

[10] C. F. Bender, (private communication).

[11] A. D. Buckingham, Adv. Chem. Phys. **12**, 107 (1967). The expressions for the first four $v_\lambda^l (0 \leq \lambda \leq 3)$ are

given by Eq. (59) of Buckingham. The induction contribution to v_4^l is given by the final equation on p. 70 of Margenau and Kestner (Ref. 12).

[12] R. M. Herman, J. Chem. Phys. **44**, 1346 (1966); H. Margenau and N. R. Kestner, *The Theory of Intermolecular Forces*, 2nd ed. (Pergamon, Oxford, 1971), p. 72.

[13] H. J. Kolker and M. Karplus, J. Chem. Phys. **39**, 2011 (1963).

[14] A. Dalgarno, Adv. Phys. **11**, 281 (1962).

[15] R. F. W. Bader, I. Keaveny, and P. E. Cade, J. Chem. Phys. **47**, 3381 (1967).

[16] D. E. Stogryn and A. P. Stogryn, Mol. Phys. **11**, 371 (1966).

[17] A. M. Arthurs and A. Dalgarno, Proc. R. Soc. Lond. A **256**, 540 (1960).

[18] W. N. Sams and D. J. Kouri, J. Chem. Phys. **51**, 5814 (1969); E. F. Hayes, C. A. Wells, and D. J. Kouri, Phys. Rev. A **4**, 1017 (1971).

[19] The partial cross sections $\sigma^J (j \to j')$ were calculated at even values of J for both even and odd parities. The partial cross sections at odd values of J were found by graphically interpolating the even-J results.

[20] A preliminary account of this work was reported by L. A. Collins and N. F. Lane, Bull. Am. Phys. Soc. **19**, 1191 (1974).